J. Fluid Mech. (1993), *vol.* 249, *pp.* 185–206

The effect of residual axial gravity on the stability of liquid columns subjected to electric fields

By HELIODORO GONZÁLEZ AND ANTONIO CASTELLANOS

Departamento de Electrónica y Electromagnetismo, Universidad de Sevilla, 41012 Seville, Spain

(Received 19 December 1991 and in revised form 19 October 1992)

The stability criterion for almost cylindrical dielectric liquid bridges subjected to axial electric fields in the presence of residual axial gravity is obtained. In its absence, a perfectly cylindrical equilibrium solution is allowed for all values of the relevant parameters, which are the slenderness of the liquid bridge, the electrical Bond number and the relative permittivity between the outer and inner media. This basic solution is unstable beyond a critical slenderness which varies with the electrical parameters (González *et al.* 1989). The destabilization takes place axisymmetrically. The inclusion of the gravitational Bond number as a new, small parameter may be treated by means of the Lyapunov–Schmidt Method, a well-known projection technique that gives the local bifurcation diagram relating the admissible equilibrium amplitudes for the liquid bridge and the aforementioned parameters. As in the absence of applied electric field, the gravitational Bond number breaks the *pitchfork* diagram into two isolated branches of axisymmetric equilibrium solutions. The stable one has a turning point whose location determines the new stability criterion. Quantitative results are presented after solving the resulting set of linear recursive problems by means of the method of lines.

1. Introduction

The instability of liquid bridges has been investigated extensively in the last ten years, particularly in the context of microgravity applications, e.g. the floating-zone processing technique to produce large-diameter single crystals. More recently it has been shown that an axial electric field may have a strongly stabilizing effect in non-rotating/rotating isothermal cylindrical liquid bridges (González *et al.* 1989; González & Castellanos 1990). The stabilization is due to dielectric forces acting along the liquid column free interface. To this end the action of Coulomb forces originating from bulk and/or interface free charges must be avoided. This may be easily achieved if we apply an a.c. electric field with a period much shorter than the typical charge relaxation time, ϵ/c, with ϵ the electrical permittivity and c the electrical conductivity of the liquid. For melts of highly insulating materials (glasses, rocks) the industrial frequency (50 Hz) is high enough and the application of a longitudinal electric field could have a beneficial effect on the processing of these materials, both on earth and in outer space.

Imperfections of cylindrical columns are always present in experiments irrespective of whether they are performed in satellites or on earth. On earth and for long liquid columns compared to the capillary length, an outer bath of an isodense liquid has to be used to compensate for the gravity effects. Unless the temperature

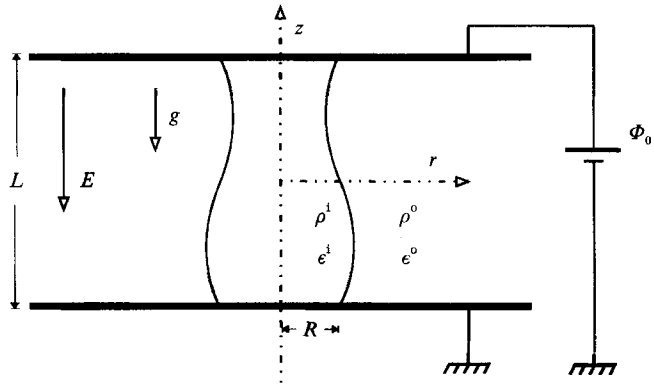

FIGURE 1. Schematic of the dielectric liquid bridge subjected to a potential difference Φ_0.

is carefully controlled, small differences in densities will be present. This was the case of the experiments performed in our laboratory (González *et al.* 1989) and we were interested in including the effect of residual axial gravity to account for the measured experimental data. In satellites the residual accelerations and a reduced but non-zero gravity also limit the possibility of having perfectly cylindrical liquid bridges.

The effect of axial residual gravity in the absence of the electric field has been considered by several authors (Coriell & Cordes 1977; Vega & Perales 1983), and it was concluded that it has a severe destabilizing influence. Thus, if we are interested in the description of liquid bridges, whatever the forces acting upon them, we must address the problem of the effect of the residual gravity on their stability.

From the mathematical point of view, the inclusion of the gravitational Bond number as a new, small parameter leads to a singular problem if we look for a perturbative solution in this parameter. However, it is possible to apply a general and powerful technique, the so-called Lyapunov–Schmidt reduction, that gives, in a natural way, the bifurcation diagram for the liquid bridge both with and without residual gravity. In the former case, information about the new stability criterion comes from the local nature of the bifurcation. Other imperfections, apart from a residual axial gravity, have been investigated using this method, e.g. eccentricity and differing radii of the anchoring disks. However, the inclusion of an electric field requires a non-trivial extension of the Lyapunov–Schmidt technique that we present in this work. The main difficulty comprises the consideration of more general Hilbert spaces where the nonlinear problem is defined as well as the treatment of nonlinear boundary conditions.

2. Formulation of the problem

The physical system under investigation is a dielectric liquid bridge between parallel electrodes, anchored at two equal-radius coaxial disks with free contact angles. We constrain the liquid volume to be that of a perfect cylinder, $V = \pi R^2 L$, where R is the disk radius and L the distance between the electrodes (see figure 1). These are considered wide enough to neglect any border effect when a constant potential difference Φ_0 is applied.

As we are interested in microgravity conditions, like those achieved in a space laboratory, with a reduced gravity level, or using the plateau tank technique in a terrestrial laboratory, i.e. using an almost isodense immiscible bath, we restrict ourselves to small gravitational Bond numbers, defined by $B = (\rho^i - \rho^o) g R^2/\sigma$, ρ^i and

ρ^{o} being the inner and outer fluid densities, σ the surface tension between these fluids and g the acceleration due to gravity.

The system is assumed to be formed by incompressible, homogeneous and charge-free liquids. Thus the electric forces that appear are of dielectric origin at the interface. No electrostriction effect need be considered.

Static configurations must satisfy the Navier–Stokes equations with zero velocity field and no time dependence giving

$$p+\rho g z = \Pi \equiv \text{constant}, \tag{1}$$

where p denotes the pressure (modified by the electrostrictive effect of the electric field), z is the axial coordinate and Π takes two different values for each medium that we will call 'effective pressures'.

The electromagnetic problem reduces to the solution of the Laplace equation for the electric potential ϕ in both media. The interface between them is described by

$$F(r,z) \equiv r - f(z) = 0, \tag{2}$$

provided that only axisymmetric equilibrium shapes are admissible. At this surface we have to satisfy the Young–Laplace equation, augmented by the dielectric forces which are normal to the interface because of the absence of free charges. The complete set of partial nonlinear differential equations in non-dimensional form satisfied by the interfacial shape function $f(z)$, and the electric potential $\phi(r,z)$ is

$$\nabla^2\phi = 0, \tag{3}$$

$$\Delta\Pi + Bz + \tfrac{1}{2}\chi\Delta[\epsilon(\nabla\phi)^2] - \frac{\chi}{|\nabla F|^2}\Delta[\epsilon(\nabla F\cdot\nabla\phi)^2] + \nabla\cdot\boldsymbol{n} = 0, \tag{4}$$

$$V = \pi\int_{-\Lambda}^{\Lambda} \mathrm{d}z f^2, \tag{5}$$

along with the boundary conditions:

$$f(\pm\Lambda) = 1, \tag{6}$$

$$\phi(r,\Lambda) = 1, \quad \phi(r,-\Lambda) = 0, \tag{7}$$

$$\frac{\partial\phi}{\partial r} = 0 \quad \text{at } r = 0, \tag{8}$$

$$\lim_{r\to\infty}\phi = z+\Lambda, \tag{9}$$

$$\Delta\phi = 0, \tag{10}$$

$$\nabla F\cdot\Delta(\epsilon\nabla\phi) = 0, \tag{11}$$

where $\boldsymbol{n}$ is the outward normal vector to the interface defined as $\boldsymbol{n} \equiv \nabla F/|\nabla F|$ evaluated at $F = 0$ and the notation Δ means the jump of a quantity across the interface, also in the outward direction. These equations are made non-dimensional by scaling lengths by R, the electric field by its value for $r\to\infty$, $E_\infty = \Phi_0/L$, the pressure by the capillary jump across the interface σ/R, and permittivities by that of the inner medium ϵ^{i}. Four non-dimensional parameters appear in the above equations: the slenderness, $\Lambda \equiv L/2R$, the gravitational Bond number already introduced, the relative permittivity of the outer to the inner medium, $\beta \equiv \epsilon^{o}/\epsilon^{i}$, and the electric Bond number, $\chi \equiv \epsilon^{i}\Phi_0^2 R/\sigma L^2$. Notice that the non-dimensional permittivity is in general written as ϵ, but β stands for the outer medium and is unity for the inner one, i.e. $\Delta\epsilon = \beta - 1$.

The constraint upon the liquid bridge volume, equation (5), has been considered as a governing equation to match the number of unknowns and equations. It is closely related to the jump in the pressure $\Delta\Pi$.

3. Cylindrical solution and its stability

Let us put the above set of equations in operational form as $\mathscr{F}(\boldsymbol{x}, \eta) = 0$, where $\mathscr{F}$ is an operator acting on a functional space $\mathscr{B}_1$ whose elements are

$$\boldsymbol{x} = (\phi^{\mathrm{i}}(r,z), \phi^{\mathrm{o}}(r,z), f(z), \Delta\Pi). \tag{12}$$

The components of this vector must satisfy the boundary conditions (6)–(11). The symbol η denotes any parametrical dependence of the operator that we might emphasize.

If $B = 0$ the system has as a simple closed solution

$$\boldsymbol{x}_{\mathrm{c}} = (z+\Lambda, z+\Lambda, 1, -1-\tfrac{1}{2}\chi\Delta\epsilon), \tag{13}$$

that represents a cylindrical liquid bridge subjected to an uniform electric field. Now we look for other solutions close to $\boldsymbol{x}_{\mathrm{c}}$ by perturbing it slightly, $\boldsymbol{x} = \boldsymbol{x}_{\mathrm{c}} + \varepsilon\boldsymbol{x}_0$, where ε is a small amplitude of deformation and

$$\boldsymbol{x}_0 = (\phi_0^{\mathrm{i}}(r,z), \phi_0^{\mathrm{o}}(r,z), f_0(z), \Delta\Pi_0). \tag{14}$$

Substituting this into the general equations (3)–(11) and retaining only first-order terms in ε we have $\boldsymbol{A}\boldsymbol{x}_0 = 0$, where $\boldsymbol{A}$ is the linear part of $\mathscr{F}$ at $\boldsymbol{x}_{\mathrm{c}}$, expressed by

$$\boldsymbol{A} = \begin{pmatrix} -\nabla^2 & 0 & 0 & 0 \\ 0 & -\nabla^2 & 0 & 0 \\ -(2\Lambda\chi\Delta\epsilon)\,\partial/\partial z & 0 & 1+\partial^2/\partial z^2 & -1 \\ 0 & 0 & -\int_{S_1} \mathrm{d}S & 0 \end{pmatrix}, \tag{15}$$

and now $\boldsymbol{x}_0$ must verify the linearized boundary conditions

$$\phi_0(r, \pm\Lambda) = 0, \tag{16}$$

$$\phi_0(0,z) = O(1), \quad \lim_{r\to\infty} \phi_0(r,z) = 0, \tag{17}$$

$$\Delta\phi_0 = 0, \tag{18}$$

$$\Delta\left(\epsilon\frac{\partial\phi_0}{\partial r}\right) - \frac{\Delta\epsilon}{2\Lambda}\frac{\partial f_0}{\partial z} = 0, \tag{19}$$

$$f_0(\pm\Lambda) = 0. \tag{20}$$

This homogeneous problem has a non-trivial solution only for selected values of Λ, β and χ, called bifurcation points in the three-dimensional parameter space. It has been shown by González *et al.* (1989) that the bifurcation points form an infinite set of nested non-intersecting surfaces in the parameter space defined implicitly by one of the following two equations:

$$S_-(\chi,\beta,\Lambda) \equiv \sum_{\substack{n=1 \\ \text{odd}}}^{\infty} q_n^{-1} = 0, \tag{21}$$

$$S_+(\chi,\beta,\Lambda) \equiv \tfrac{1}{2}q_0^{-1} + \sum_{\substack{n=2 \\ \text{even}}}^{\infty} q_n^{-1} = 0, \tag{22}$$

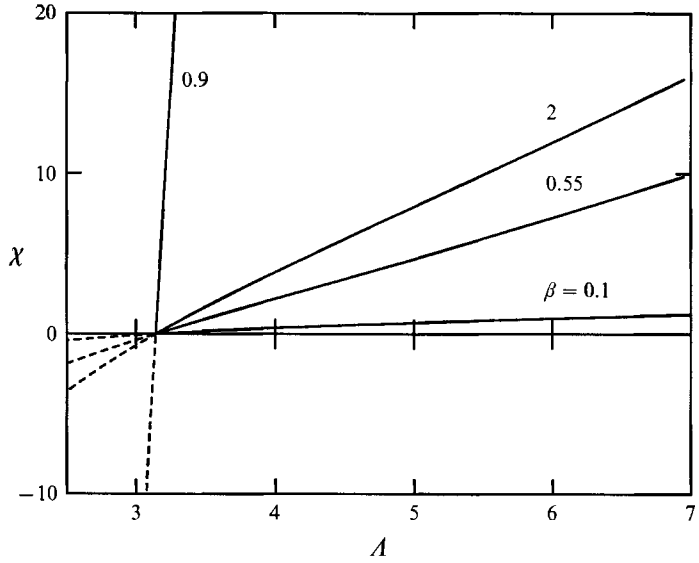

FIGURE 2. Stability curves in the (χ, Λ)-plane for different representative values of the permittivity ratio β. The stable regions in the parameter space are those above the curves. Negative values of χ are plotted with dashed lines to indicate that they have no physical meaning.

where
$$q_n(\beta, \Lambda, \chi) = 1 - x_n^2 + \frac{\chi(\Lambda\epsilon)^2 x_n}{H_0(\beta, x_n)}, \tag{23}$$

with $x_n \equiv n\pi/2\Lambda$ and $H_0(\beta, x_n) \equiv -\beta[K_1(x_n)K_0(x_n)] - [I_1(x_n)/I_0(x_n)]$, being I_0, I_1, K_0 and K_1 modified Bessel functions. In the cited reference, equations (21) and (22) were presented in a slightly different form. Here we use a more compact expression in order to infer further results in this section.

The slenderness is shown to be an ordering parameter for the infinite set of bifurcation surfaces. Only that of least Λ (corresponding to a zero of S_-) represents a transition from stability to instability of the cylindrical solution. We denote this bifurcation surface by $\chi_0(\beta, \Lambda)$, which is plotted in figure 2 for several values of β, including the experimentally tested case of $\beta = 0.55$. We have selected these values aiming to summarize the behaviour of the stability curves presented in the above-mentioned work. Notice that we have plotted the curves including negative values of χ, although only positive χ are physically admissible from its definition. Later on we will see how these points serve to construct the stability curves for $B \neq 0$.

It is possible to find the asymptotic behaviour of $\chi_0(\beta, \Lambda)$ as Λ goes to infinity from that of the singular points of S_-. This function diverges for every set of parameters giving $q_n = 0$, $n = 1, 3, \ldots$, which will be represented by $\chi_n(\beta, \Lambda)$. Between two consecutive singular points there exists one and only one zero of S_-. In particular, $q_1 = 0$ and $q_3 = 0$ give upper and lower bounds to the stability curve, i.e. $\chi_1 < \chi_0 < \chi_3$. If we look for the asymptotic behaviour of χ_n as $\Lambda \to \infty$ from that of the intervening modified Bessel functions for small arguments we obtain the dominant behaviour

$$\chi_n(\beta, \Lambda) \sim C(\Lambda)\frac{\beta}{|\Delta\epsilon|}\Lambda^2, \tag{24}$$

where C is bounded and varies as slowly as $1/\ln(n\pi/2\Lambda)$. Obviously this latter expression is also valid for the asymptotic behaviour of χ_0. In figure 2 this behaviour is not apparent because the range of Λ of relevance in the experiment is limited.

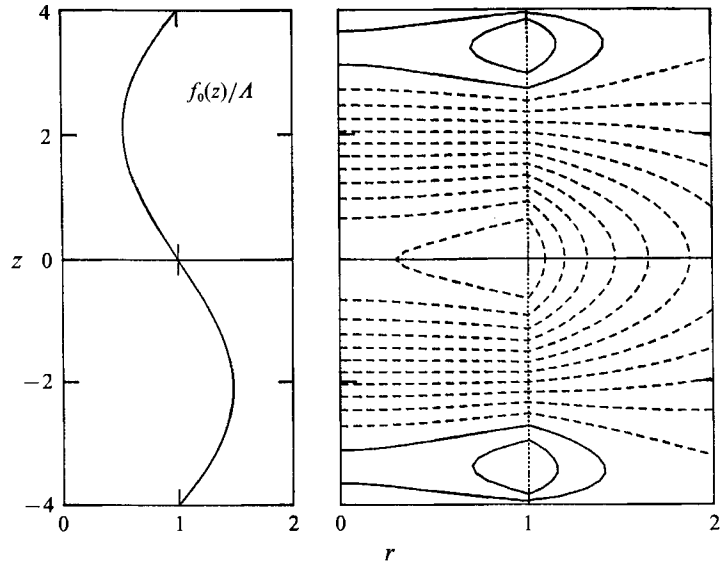

FIGURE 3. Shape $f_0(z)$ and equipotential lines of the function $\phi_0(r,z)$, the bifurcating family at $\chi = \chi_0$ for $\beta = 0.55$ and $\Lambda = 4$. In the equipotential map: ——, positive values of the electric potential; – – –, negative values of the electric potential.

The bifurcating family is

$$\begin{Bmatrix} \phi_0^{\mathrm{i}}(r,z) \\ \phi_0^{\mathrm{o}}(r,z) \end{Bmatrix} = -\frac{\Delta\epsilon}{2\Lambda} \sum_{\substack{n=1 \\ \text{odd}}}^{\infty} \begin{Bmatrix} I_0(x_n r)/I_0(x_n) \\ K_0(x_n r)/K_0(x_n) \end{Bmatrix} \frac{\sin[x_n(z+\Lambda)]}{H_0(\beta, x_n)\, q_n(\beta, \Lambda, \chi_0)}, \tag{25}$$

$$f_0(z) = \sum_{\substack{n=1 \\ \text{odd}}}^{\infty} \frac{\cos[x_n(z+\Lambda)]}{q_n(\beta, \Lambda, \chi_0)}, \tag{26}$$

$$\Delta\Pi_0 = 0. \tag{27}$$

The electric potentials at the critical point are symmetric with respect to the middle plane $z = 0$, whereas the interface shape is anti-symmetric. The interface shape and some equipotentials are plotted in figure 3 for $\beta = 0.55$ and $\Lambda = 4$.

It is convenient to describe the summation technique for series like those defining $f_0(z)$ or $\phi_0(r,z)$ and their derivatives evaluated at the interface, which are used later in this paper (see Appendix A). Let us fix our attention on $f_0(z)$. For $n \to \infty$ the coefficients q_n^{-1} have an asymptotic behaviour given by $a_1/x_n^2 + a_2/x_n^3 + a_3/x_n^4 + \ldots \equiv q_{n,\infty}^{-1}$ for some easily determined coefficients $a_1, a_2, a_3, \ldots$. If we substitute the original series by

$$\begin{aligned} f_0(z) \simeq f_0^N(z) &\equiv \sum_{\substack{n=1 \\ \text{odd}}}^{N} q_n^{-1} \cos[x_n(z+\Lambda)] + \sum_{\substack{n=N+2 \\ \text{odd}}}^{\infty} q_{n,\infty}^{-1} \cos[x_n(z+\Lambda)] \\ &= \sum_{\substack{n=1 \\ \text{odd}}}^{N} (q_n^{-1} - q_{n,\infty}^{-1}) \cos[x_n(z+\Lambda)] + \sum_{\substack{n=1 \\ \text{odd}}}^{\infty} q_{n,\infty}^{-1} \cos[x_n(z+\Lambda)], \end{aligned} \tag{28}$$

where N is an arbitrary odd number, the error will depend on both the number of terms actually included in $q_{n,\infty}^{-1}$ and on N. Retaining terms up to the order x_n^{-4} the error is

$$f_0(z) - f_0^N(z) = \sum_{\substack{n=N+2 \\ \text{odd}}}^{\infty} (q_n^{-1} - q_{n,\infty}^{-1}) \cos[x_n(z+\Lambda)] \sim O(N^{-4}), \tag{29}$$

estimated by means of the integral criterion for summation applied to a series whose terms are of order $1/n^5$. If $N \approx 100$ we obtain at least an accuracy of seven decimal figures.

The final infinite series in (28) are of the type $\sum_n \cos(ny)/n^p$, $p = 2, 3, 4$. For p odd, they are easily expressed in closed form. On the other hand, for p even, we can transform them into exponentially convergent series using residues summation techniques (see e.g. Collin 1991). In the case $p = 3$ we put

$$\sum_{n=1}^{\infty} \frac{\cos(ny)}{n^3} = \sum_{n=1}^{\infty} \frac{\cos(ny)}{n^3}[1-\tanh(ns)] + \sum_{n=1}^{\infty} \frac{\cos(ny)\tanh(ns)}{n^3}, \tag{30}$$

where $0 < s < 1$. The first series on the right-hand side of (30) converges exponentially. For the second one we consider the function of complex variable z defined by

$$g(z) = \frac{e^{izy}\tanh(zs)}{z^3} \frac{1}{e^{2\pi zi}-1}. \tag{31}$$

One has

$$\oint_{\Gamma} g(z)\,dz = 2\pi i \sum_{\alpha} \mathrm{Res}_{z=z_\alpha} g(z) = 0, \tag{32}$$

where Γ is a circular integration contour of radius going to infinity and z_α are the poles of $g(z)$ where the residues of the function are calculated. The null value of the integral comes from the limit of the integrand as $|z| \to \infty$. There exist simple poles at $z = n$ (n integer) for all $n \neq 0$ and at $z = (2m+1)\pi i/2s$ for all m integer. At $z = 0$ we have a third-order pole. Residues at real axis poles generate double the series that we need to calculate and residues at imaginary axis poles gives another series with exponential convergence.

The method fails for values of y close to 0 or 2π. In these cases it is better to use an approximation based upon a Laurent expansion of $\sum_{n=1}^{\infty} \cos(ny)/n = -\ln[2\sin(\frac{1}{2}y)]$ which is twice integrated to give the corresponding expansion of $\sum_{n=1}^{\infty} \cos(ny)/n^3$.

All of these procedures are applicable to the calculus of any functional series of the type $\mathrm{cn}_{2p+1}(y) \equiv \sum_{n=1}^{\infty} \cos(ny)/n^{2p+1}$ and $\mathrm{sn}_{2p}(y) \equiv \sum_{n=1}^{\infty} \sin(ny)/n^{2p}$. On the other hand the functions $\mathrm{cn}_{2p}(y)$ and $\mathrm{sn}_{2p+1}(y)$ are polynomials of order $2p$ in the argument y.

4. The Lyapunov–Schmidt method

The main intent of this paper is to extend the stability analysis from $B = 0$, presented by González *et al.* (1989), to cases where B, although small, is non-zero. Using regular perturbation techniques based directly on the parameter B in the form $\boldsymbol{x} = \boldsymbol{x}_c + B\boldsymbol{x}_B + B^2\boldsymbol{x}_{B^2} + \ldots$ and $\chi = \chi_0 + B\chi_B + \ldots$, we readily find with an analysis similar to that of González that the first-order solution is

$$\begin{Bmatrix} \phi_B^{\mathrm{in}} \\ \phi_B^{\mathrm{ex}} \end{Bmatrix} = -\frac{\Delta\epsilon}{\Lambda^2} \sum_{\substack{n=1 \\ \mathrm{odd}}}^{\infty} \frac{1/x_n^2 - k}{H_0(\beta, x_n)\, q_n} \begin{Bmatrix} I_0(x_n r)/I_0(x_n) \\ K_0(x_n r)/K_0(x_n) \end{Bmatrix} \sin[x_n(z+\Lambda)], \tag{33}$$

$$f_B = \frac{2}{\Lambda} \sum_{\substack{n=1 \\ \mathrm{odd}}}^{\infty} (1/x_n^2 - k)\, q_{0n}^{-1} \cos[x_n(z+\Lambda)], \tag{34}$$

$$\Delta\Pi_B = 0, \tag{35}$$

where
$$k \equiv \left(\sum_{\substack{n=1 \\ \text{odd}}}^{\infty} x_n^{-2} q_n^{-1} \right) \Big/ \left(\sum_{\substack{n=1 \\ \text{odd}}}^{\infty} q_n^{-1} \right). \tag{36}$$

Putting $\chi = 0$ and considering $\Lambda < \pi$, we recover previous results without an imposed electric field (Martínez 1983):

$$f_B(z) = \Lambda \left[\frac{\sin z}{\sin \Lambda} - \frac{z}{\Lambda} \right]. \tag{37}$$

This method fails because k goes to infinity as χ goes to χ_0 (or Λ goes to π in the latter special case (37)). This exhibits the singular nature of the problem. We must regard $\boldsymbol{x}_B$ as the outer solution evaluated far from the critical point.

These features are common to the already studied problem of almost cylindrical isorotating liquid bridges for small gravitational Bond numbers (Vega & Perales 1983). In that work and other related situations (Perales 1987; Perales, Sanz & Rivas 1990) the Lyapunov–Schmidt method was successfully applied to obtain the stability behaviour for $B \neq 0$ by means of a regular perturbation technique. This *projection* method enables us to find the bifurcation equation corresponding to a nonlinear partial differential problem, i.e. a relation between the parameters and the amplitudes of the bifurcating families for which there exists a solution to the nonlinear problem. In our case at $\chi_0(\beta, \Lambda)$ the bifurcating family is a single-parameter one, ϵ being the only amplitude.

4.1. *Description*

Let us fix β and Λ, so that the symbol η only represents χ and B. We look for solution sets $(\boldsymbol{x}, \chi, B)$ of $\mathscr{F}(\boldsymbol{x}, \chi, B) = 0$ which are a local extension of the bifurcation set $(\boldsymbol{x}_c, \chi_0, 0)$. Obviously the operator $\mathscr{F}$ evaluated at this latter set is not invertible and we cannot apply directly the implicit function theorem to obtain the desired local extension. Nevertheless, we can overlook this difficulty because $\boldsymbol{A}$, the linear part of $\mathscr{F}$, is a Fredholm operator since it has the following three defining properties: (i) its kernel has finite dimension; (ii) its adjoint operator, $\boldsymbol{A}^*$, has a kernel with the same dimension, and (iii) the original space $\mathscr{B}_1$ can be decomposed into a direct sum of the kernel of $\boldsymbol{A}$ and its orthogonal subspace, as well as the final space, denoted as $\mathscr{B}_2$, can be decomposed into a direct sum of the domain of $\boldsymbol{A}$ and that orthogonal to it. In our case $\dim(\mathrm{Ker}(\boldsymbol{A})) = 1$. On the other hand defining the inner product as

$$\langle \boldsymbol{x}_1, \boldsymbol{x}_2 \rangle \equiv \chi_0 \int_{V_i} \mathrm{d}V \, \phi_1^i \phi_2^i + \beta \chi_0 \int_{V_o} \mathrm{d}V \, \phi_1^o \phi_2^o + \int_{S_1} \mathrm{d}S f_1 f_2 + \Delta \Pi_1 \Delta \Pi_2, \tag{38}$$

with V_i and V_o the inner and outer regions respectively, and S_1 its common boundary, it may be shown that the operator $\boldsymbol{A}$ is self-adjoint, so that the second property holds and the image of $\boldsymbol{A}$ coincides with the kernel of $\boldsymbol{A}^*$. Thus we can perform the decomposition $\boldsymbol{x} = \varepsilon \boldsymbol{x}_0 + \boldsymbol{x}_\perp$ in both isomorphous functional spaces $\mathscr{B}_1$ and $\mathscr{B}_2$, with $\boldsymbol{x}_0$ belonging to $\ker(\boldsymbol{A})$ and $\boldsymbol{x}_\perp$ to its orthogonal set. The important feature about Fredholm operators is that the equation $\boldsymbol{A}\boldsymbol{x} = \boldsymbol{y}$ is equivalent to the set $\boldsymbol{A}\boldsymbol{x}_\perp = (\mathscr{I} - \mathscr{P})\boldsymbol{y}$, $\mathscr{P}\boldsymbol{y} = 0$, where $\mathscr{I}$ is the identity operator in $\mathscr{B}_2$ and $\mathscr{P}$ is the projection operator onto the orthogonal subspace to the image of $\boldsymbol{A}$, so that $\mathscr{I} - \mathscr{P}$ projects any vector belonging to $\mathscr{B}_2$ onto the image of $\boldsymbol{A}$. Decomposing the original equation in the form $\mathscr{F}(\boldsymbol{x}, \chi, B) = \boldsymbol{A}\boldsymbol{x} + \mathscr{R}(\boldsymbol{x}, \chi, B) = 0$ and using the result about Fredholm operators we arrive to

$$\boldsymbol{A}\boldsymbol{x}_\perp = -(\mathscr{I} - \mathscr{P})\mathscr{R}(\boldsymbol{x}_\perp - \varepsilon \boldsymbol{x}_0, \chi, B), \tag{39}$$

$$\mathscr{P}\mathscr{R}(\boldsymbol{x}_\perp + \varepsilon \boldsymbol{x}_0, \chi, B) = 0, \tag{40}$$

where the vector $\boldsymbol{x}$ has been explicitly decomposed. The problem is now solvable by the implicit function theorem because $\boldsymbol{A}$ is not singular when acting on the space orthogonal to its kernel and the right-hand side of (39) belongs to its image space.

The above description of the Lyapunov–Schmidt method follows that of Myshkis *et al.* (1986). Another useful version of the method is directly introduced in Vega & Perales (1983). This latter work uses the fact that the projection of $\mathscr{R}$ onto the subspace orthogonal to the image of $\boldsymbol{A}$ can be expressed in the basis of the kernel of $\boldsymbol{A}$, provided that $\boldsymbol{A}$ is a self-adjoint operator. Thus we have

$$-\mathscr{P}\mathscr{R}(\boldsymbol{x}_\perp+\varepsilon\boldsymbol{x}_0,\chi,B)=\psi(\chi,B,\varepsilon)\,\boldsymbol{x}_0, \tag{41}$$

with ψ a scalar dependent on the parameters and the amplitude of the bifurcating family. The equivalent problem is now

$$\mathscr{F}(\boldsymbol{x}_\perp,\chi,B)+\psi\boldsymbol{x}_0=0, \tag{42}$$

$$\langle\boldsymbol{x}_0,\mathscr{R}(\boldsymbol{x}_\perp+\varepsilon\boldsymbol{x}_0,\chi,B)\rangle=0. \tag{43}$$

The second equation can be read as $\psi(\varepsilon,\chi,B)=0$, which is the bifurcation equation.

In practice we solve this final problem by expanding $\boldsymbol{x}_\perp\equiv(\varphi^{\mathrm{i}},\varphi^{\mathrm{o}},u,\Delta P)$, $\mathscr{R}$ and ψ in the parameters $\bar{\chi}\equiv\chi-\chi_0$, ε and B:

$$\begin{Bmatrix}\boldsymbol{x}_\perp\\ \mathscr{R}\\ \psi\end{Bmatrix}=\sum_{i+j+k>0}\bar{\chi}^i\varepsilon^jB^k\begin{Bmatrix}\boldsymbol{x}_{\perp,ijk}\\ \mathscr{R}_{ijk}\\ \psi_{ijk}\end{Bmatrix}. \tag{44}$$

This yields an infinite set of linear non-homogeneous recursive problems whose general form is

$$\nabla^2\varphi_{ijk}-\psi_{ijk}\phi_0=0, \tag{45}$$

$$\varphi_{ijk}(r,\pm\Lambda)=0, \tag{46}$$

$$\varphi_{ijk}(0,\theta,z)=O(1),\quad\lim_{r\to\infty}\varphi_{ijk}(r,z)=0, \tag{47}$$

$$\Delta\varphi_{ijk}=h^{(1)}_{ijk}(z), \tag{48}$$

$$\Delta\left(\epsilon\frac{\partial\varphi_{ijk}}{\partial r}\right)-\frac{\Delta\epsilon}{2\Lambda}\frac{\partial u_{ijk}}{\partial z}=h^{(2)}_{ijk}(z), \tag{49}$$

$$\left(1+\frac{\mathrm{d}^2}{\mathrm{d}z^2}\right)u_{ijk}-2\Lambda\chi_0\Delta\left(\epsilon\frac{\partial\varphi_{ijk}}{\partial z}\right)-\pi_{ijk}-\psi_{ijk}f_0(z)=h^{(3)}_{ijk}(z), \tag{50}$$

$$u_{ijk}(\pm\Lambda)=0, \tag{51}$$

$$\int_{-\Lambda}^{\Lambda}\mathrm{d}z\,u_{ijk}=\int_{-\Lambda}^{\Lambda}\mathrm{d}z\,h^{(4)}_{ijk}, \tag{52}$$

where the functions $h^{(l)}_{ijk}(z)$, $l=1,2,3,4$, come from the expansion of the nonlinear part of the operator and boundary conditions. They depend on the lower-order solutions, i.e. $\boldsymbol{x}_{\perp,i-1,j,k}$, $\boldsymbol{x}_{\perp,i,j-1,k}$, $\boldsymbol{x}_{\perp,i,j,k-1}$, …, $\boldsymbol{x}_0$. In Appendix A we present a list of the functions $h^{(l)}_{ijk}$ for the orders just necessary to obtain the local bifurcation diagram, as discussed in the next paragraph.

Along with equations (45)–(52), we have the relation between ψ_{ijk} and $\mathscr{R}_{ijk}$:

$$\psi_{ijk}\langle\boldsymbol{x}_0,\boldsymbol{x}_0\rangle=-\langle\boldsymbol{x}_0,\mathscr{R}_{ijk}\rangle. \tag{53}$$

We must still determine the specific relation between $\mathscr{R}_{ijk}$ and the functions $h^{(l)}_{ijk}(z)$. This will be done in §4.3.

4.2. *Some symmetry properties*

Before attempting to compute recursively the solution to every linear problem, it is better to take advantage of some properties arising from the symmetries that leave invariant the full set of extended governing equations and boundary conditions, (42), (43) and (6)–(11). The transformation

$$z \to -z, \quad \varepsilon \to -\varepsilon, \quad u \to u, \quad \varphi \to -\varphi, \quad B \to -B, \quad \psi \to -\psi, \tag{54}$$

leads to the same problem. This implies

$$u_{ijk}(-z) = (-1)^{j+k+1} u_{ijk}(z), \quad \varphi_{ijk}(r,-z) = (-1)^{j+k+1} \varphi_{ijk}(r,z), \tag{55}$$

$$p_{ijk} = 0 \quad \text{if } j+k \text{ is odd}, \tag{56}$$

$$\psi_{ijk} = 0 \quad \text{if } j+k \text{ is even}, \tag{57}$$

as well as

$$h^{(1)}_{ijk}(-z) = (-1)^{j+k+1} h^{(1)}_{ijk}(z), \quad h^{(2)}_{ijk}(-z) = (-1)^{j+k+1} h^{(2)}_{ijk}(z), \tag{58}$$

$$h^{(3)}_{ijk}(-z) = (-1)^{j+k} h^{(3)}_{ijk}(z), \quad h^{(4)}_{ijk}(-z) = (-1)^{j+k} h^{(4)}_{ijk}(z). \tag{59}$$

The result about ψ allows us to anticipate the type of bifurcation:

$$\varepsilon(\psi_{110}\bar{\chi} + \psi_{030}\varepsilon^2) + \psi_{001} B + \ldots = 0. \tag{60}$$

For $B = 0$ we have a *pitchfork* bifurcation and the gravitational Bond number breaks it into two isolated branches of solutions. A quantitative plot of (60) for both cases will be shown in a later section.

4.3. *The compatibility condition*

Here we obtain the expansion coefficients for ψ from (53). In that equation the factor $\langle \boldsymbol{x}_0, \boldsymbol{x}_0 \rangle$ can be omitted because it does not depend on the subindexes and it is common to every term in the expansion of ψ.

Some care must be taken in order to evaluate the inner product because it is defined in the Hilbert space that verifies the linearized boundary conditions (16)–(20). In particular, we have to relate the functions $h^{(l)}_{ijk}$ with $\mathscr{R}_{ijk}$. To make this we consider the transformation

$$\varphi^{\mathrm{i}}_{ijk}(r,z) = \hat{\varphi}^{\mathrm{i}}_{ijk}(r,z) - g_{ijk}(r,z), \quad \varphi^{\mathrm{o}}_{ijk}(r,z) = \hat{\varphi}^{\mathrm{o}}_{ijk}(r,z), \tag{61}$$

$$u_{ijk}(z) = \hat{u}_{ijk}(z), \quad \pi_{ijk} = \hat{\pi}_{ijk}, \tag{62}$$

with

$$g_{ijk}(r,z) = [(1-r)h^{(2)}_{ijk}(z) + h^{(1)}_{ijk}(z)]\,\vartheta(z), \tag{63}$$

where $\vartheta(z)$ is a 'window function' defined as the unity for $|z| < \Lambda$ and zero otherwise. In this way we have homogeneous boundary conditions for the new unknowns. The last factor in (63) is included to maintain homogeneous boundary conditions at the electrodes after the transformation. We are now able to identify

$$\mathscr{R}_{ijk} = \left(\nabla^2 g_{ijk}, 0, h^{(3)}_{ijk} - 2\Lambda\chi_0 \frac{\mathrm{d}g_{ijk}}{\mathrm{d}z}(1,z), -\int_{S_1} \mathrm{d}S h^{(4)}_{ijk} \right). \tag{64}$$

The next step to determine ψ_{ijk} is to introduce this vector into (53). With the help of the second Green identity, the symmetry properties for g_{ijk} coming from those of $h^{(1)}_{ijk}$ and $h^{(2)}_{ijk}$, and some integrations by parts we arrive to the following compatibility condition:

$$\psi_{ijk} = \int_{-\Lambda}^{\Lambda} \mathrm{d}z \left\{ f_0 h^{(3)}_{ijk} - 4\Lambda^2\chi_0 \left[\phi_0^{\mathrm{in}} h^{(2)}_{ijk} + \left(\frac{1}{2\Lambda}\frac{\mathrm{d}f_0}{\mathrm{d}z} - \frac{\partial \phi_0^{\mathrm{in}}}{\partial r} \right) h^{(1)}_{ijk} \right] \right\}. \tag{65}$$

Looking at the bifurcation equation (60) we realize that the only linear problem to be completely solved is that of order $\bar{\chi}^0\varepsilon^2 B^0$, i.e. the system of linear non-homogeneous equations (45)–(52) particularized for $(ijk) = (020)$. The intervening non-homogeneous functions are listed in Appendix A.

5. Numerical procedure: the method of lines

We now address the problem of the numerical computation of the functions u_{020} and φ_{02}. We will drop all three subindexes through this section to make the reading easier. From symmetry considerations we know that $\psi = 0$, $u(-z) = u(z)$ and $\varphi(r, -z) = -\varphi(r, z)$ for both the inner and outer regions. The problem can be redefined in the upper half region $z \in [0, \Lambda]$ because u and φ have definite parity, so that we replace the conditions $u = \varphi = 0$ at $z = -\Lambda$ by $\mathrm{d}u/\mathrm{d}z = \varphi = 0$ at $z = 0$.

If we try to solve the problem by means of a discrete Fourier cosine transform in the variable z, as was done for the homogeneous problem by González *et al.* (1989), we readily find some trouble in evaluating the transforms of the non-homogeneous terms $h^{(i)}(z)$, because they are products of functions expressed by infinite slowly converging series. The transforms themselves are infinite series whose summation is a formidable task.

Alternatively, we propose the use of a semianalytic method known as the method of lines in the literature (Graney & Richardson 1981; Mikhail 1987). Let us consider the whole new domain $(r, z) \in [0, \infty) \times [0, \Lambda]$ decomposed into $n+1$ horizontal strips delimited by the lines $z_i = hi$, $i = 0, 1, \ldots, n+1$ with $h \equiv \Lambda/(n+1)$. At each line the functions to be found have the values $u(z_i) \equiv u_i$, $\varphi(r, z_i) \equiv \varphi_i(r)$. We have the prescribed boundary conditions $u_{n+1} = \varphi_0(r) = \varphi_{n+1}(r) = 0$. Then, we build the vectors $\boldsymbol{u} = (u_0, u_1, \ldots, u_n)$ and $\boldsymbol{\varphi}(r) = (\varphi_1(r), \varphi_2(r), \ldots, \varphi_n(r))$ as the new unknowns.

We now represent all z-derivatives of these functions by a fourth-order centred finite-difference scheme which is discussed in some detail later. The Laplace equation for the axisymmetric potential $\varphi(r, z)$,

$$\left[\frac{1}{r}\frac{\partial}{\partial r}\left(r\frac{\partial}{\partial r}\right) + \frac{\partial^2}{\partial z^2}\right]\varphi = 0, \tag{66}$$

becomes a system of linear homogeneous ordinary differential equations, expressed in matrix form as

$$[\boldsymbol{L}(r) + \boldsymbol{D}^{2\varphi}]\,\boldsymbol{\varphi}(r) = 0, \tag{67}$$

where $\boldsymbol{L}(r) \equiv (1/r)\,\partial/\partial r(r\,\partial/\partial r)\boldsymbol{I}$ ($\boldsymbol{I}$, the $n \times n$ unit matrix) and $\boldsymbol{D}^{2\varphi}$ the pentadiagonal matrix that represent the finite-difference scheme replacing the second-order z-derivative (see Appendix B).

Let $\boldsymbol{\Gamma}$ be the matrix that diagonalizes $\boldsymbol{D}^{2\varphi}$, so that $\boldsymbol{D}^{2\varphi}\boldsymbol{\Gamma} = \boldsymbol{\Gamma}\boldsymbol{A}$, with $\boldsymbol{A}$ a diagonal matrix. We define a new vector,

$$\bar{\boldsymbol{\varphi}}(r) = \boldsymbol{\Gamma}^{-1}\boldsymbol{\varphi}(r), \tag{68}$$

for which we have an uncoupled system of differential equations

$$[\boldsymbol{L}(r) + \boldsymbol{A}]\,\bar{\boldsymbol{\varphi}}(r) = 0. \tag{69}$$

Defining μ_k such that $A_{kk} = -\mu_k^2$ we have

$$\bar{\varphi}_k^{\mathrm{i}} = b_k^{\mathrm{i}}\frac{I_0(\mu_k r)}{I_0(\mu_k)}, \quad \bar{\varphi}_k^{\mathrm{o}} = b_k^{\mathrm{o}}\frac{K_0(\mu_k r)}{K_0(\mu_k)}, \tag{70}$$

as a convenient representation of the solution of the above system verifying the conditions (47). In matricial form we write for the original vector functions $\varphi^{i}(r)$, $\varphi^{o}(r)$:

$$\varphi^{i}(r) = \Gamma M_I(r)\, b^{i}, \quad \varphi^{o}(r) = \Gamma M_K(r)\, b^{o}, \tag{71}$$

where $M_I(r)$ and $M_K(r)$ are diagonal matrices whose non-zero elements are $I_0(\mu_k r)/I_0(\mu_k)$ and $K_0(\mu_k r)/K_0(\mu_k)$, respectively, and the vectors b^{i} and b^{o} are constructed with the coefficients $b_k^{i}, b_k^{o}, k = 1, 2, \ldots, n$.

The radial dependence that we have found is clearly related to the solution of the Laplace equation by the separation of variables technique, only differing in the argument of the modified Bessel functions. Notice that we have already made implicit use of the homogeneous conditions at the upper electrode and at $z = 0$ when constructing the matrix $D^{2\varphi}$. The independence of this procedure from the particular interfacial shape suggests that the method of lines is suitable for more general liquid bridge configurations.

The next step is to discretize the remaining boundary conditions at the interface. Equations (49) and (50) read

$$\Gamma(b^{o} - b^{i}) = h^{(1)}, \tag{72}$$

$$\Gamma(\beta M'_K(1)\, b^{o} - M'_I(1)\, b^{i}) - \frac{\Delta\epsilon}{2\Lambda} D^{1u} u = h^{(2)}, \tag{73}$$

where we introduce the notation $h^{(l)}$ with $l = 1, \ldots, 4$ for the vectors arising from the discretization of the corresponding functions $h^{(l)}(z)$, and D^{1u} stands for the discretization matrix of $\mathrm{d}u/\mathrm{d}z$ (see Appendix B). We use primes for derivatives with respect to a single argument.

For the pressure balance, equation (51), we have

$$(I + D^{2u})\, u - p\mathbf{1} - 2\Lambda\chi_0 \Delta\epsilon D^{1\varphi} b^{i} = h^{(3)} + \frac{\chi_0 \beta}{2\Lambda} h'^{(1)} \tag{74}$$

being D^{2u} and $D^{1\varphi}$ the discretization matrices corresponding to $\mathrm{d}^2u/\mathrm{d}z^2$ and $\partial\varphi/\partial z$ respectively, $\mathbf{1}$ the $(n+1)$-dimensional vector whose elements are all unity, and $h'^{(1)}$ the discretization of the function $\mathrm{d}h^{(1)}/\mathrm{d}z$.

Finally the integral condition (52) is discretized by means of the Simpson's integration rule, which is consistent with the fourth-order finite-difference schemes used so far. It is written as a scalar product

$$s \cdot u = s \cdot h^{(4)} \tag{75}$$

with $s = \frac{1}{3}(1, 4, 2, \ldots, 4, 2, 4, 1)$ an n-dimensional vector.

Solving for b^{i} and b^{o} from (72) and (73) as a function of u and substituting the former vector into (74) finally gives the following algebraic system of $(n+2)$ equations in the unknowns u_i and p, written with the help of block matrices:

$$\begin{pmatrix} C & \mathbf{1} \\ s^{t} & 0 \end{pmatrix} \begin{pmatrix} u \\ p \end{pmatrix} = \begin{pmatrix} h \\ \overline{s \cdot h^{(4)}} \end{pmatrix}, \tag{76}$$

with

$$C = I + D^{2u} - \chi_0 (\Delta\epsilon)^2 D^{1\varphi} \Gamma M^{-1} H_0(\beta, M)^{-1}\, \Gamma^{-1} D^{1u},$$

$$h = h^{(3)} + 2\Lambda\chi_0 \beta h'^{(1)} + 2\Lambda\chi_0 \Delta\epsilon D^{1\varphi} \Gamma M^{-1} H_0(\beta, M)^{-1} \times \{\Gamma^{-1} h^{(2)} - [H_0(\beta, M) - H_0(0, M)]\, M \Gamma^{-1} h^{(1)}\}, \tag{77}$$

where we introduce the diagonal matrices $\boldsymbol{M}$ and $\boldsymbol{H}_0(\beta, \boldsymbol{M})$, whose non-zero elements are the μ_i, $i = 1, \ldots, n$ and $H_0(\beta, \mu_i)$ respectively.

The linear system has a coefficient matrix whose elements are non-zero in general and it is actually solved by an appropriate standard routine from the IMSL package. Once we obtain $\boldsymbol{u}$ we have for the potential coefficients:

$$\boldsymbol{b}^{\text{in}} = \boldsymbol{M}^{-1}\boldsymbol{H}_0(\beta, \boldsymbol{M})^{-1}\left\{\boldsymbol{\Gamma}^{-1}\frac{\Delta\epsilon}{2\Lambda}\boldsymbol{D}^{1u}\boldsymbol{u} + \boldsymbol{h}^{(2)} - [\boldsymbol{H}_0(\beta, \boldsymbol{M}) - \boldsymbol{H}_0(0, \boldsymbol{M})]\boldsymbol{M}\boldsymbol{\Gamma}^{-1}\boldsymbol{h}^{(1)}\right\}, \quad (78)$$

$$\boldsymbol{b}^{\text{ex}} = \boldsymbol{b}^{\text{in}} + \boldsymbol{\Gamma}^{-1}\boldsymbol{h}^{(1)}. \quad (79)$$

Finally, we give some details about the discretization of the z-derivatives. The fourth-order finite-difference scheme has been selected to give enough accuracy with fewer number of lines. The centred scheme is traditionally used for the sake of stability of the numerical algorithms. As a matter of fact, a forward difference scheme makes the arguments λ_k of the modified Bessel functions complex, which does not agree with the analytical resolution of the Laplace equation. Near $z = 0$ we can still use a centred scheme because the symmetries of $u(z)$ and $\varphi(r, z)$ can be applied to consider new lines outside the interval $z \in [0, \Lambda]$ without adding new unknowns. However, at $z = \Lambda$ we cannot do the same. We thus adopted a fourth-order forward-difference scheme involving the lines z_{n+1}, z_n, z_{n-1} and z_{n-2} to represent the z-derivatives at $z = z_n$. The resulting matricial representation of the four participating derivatives can be found in Appendix B.

6. Results and discussion

We have already established the nature of the bifurcation of the cylindrical solution as being of a pitchfork type, as well as the breaking effect of the gravitational Bond number on the bifurcation diagram, based exclusively upon symmetry arguments. On the other hand, we know that the cylindrical solution ($B = 0, \epsilon = 0$) is stable for $\chi > \chi_0$ and unstable for $\chi < \chi_0$. These features are now completed.

6.1. *The case* $B = 0$

The most relevant information obtained from the subsequent numerical computation of the coefficients ψ_{110} and ψ_{030} is that the bifurcation is subcritical for all tested values of β and Λ, i.e. $\psi_{030}/\psi_{110} < 0$. In figure 4 we show the bifurcation diagram for the case $\beta = 0.55$ and $\Lambda = 4$. Physically the liquid bridge needs greater electric fields to stabilize slightly deformed shapes. The represented amplitude has been renormalized as

$$\varepsilon = \left[\frac{1}{2\Lambda}\int_{-\Lambda}^{\Lambda} \mathrm{d}z(f(z) - 1)^2\right]^{\frac{1}{2}}, \quad (80)$$

to deal with a parameter available in practice.

With the help of the factorization theorem (Iooss & Joseph 1980) we can establish the stability of the cylinder to small but finite perturbations from this static study. According to this theorem, two families of solutions change their stability at a double point, as it is $\varepsilon = 0$, $\chi = \chi_0$, if the bifurcation is subcritical. Thus the parabolic branches represent unstable equilibria and divide the (ε, χ)-plane into two regions: the inner region is the cylindrical solution attraction domain, while initial deformations with amplitudes lying on the outer region evolve to other equilibria, presumably to the breaking into two separate drops attached to each electrode.

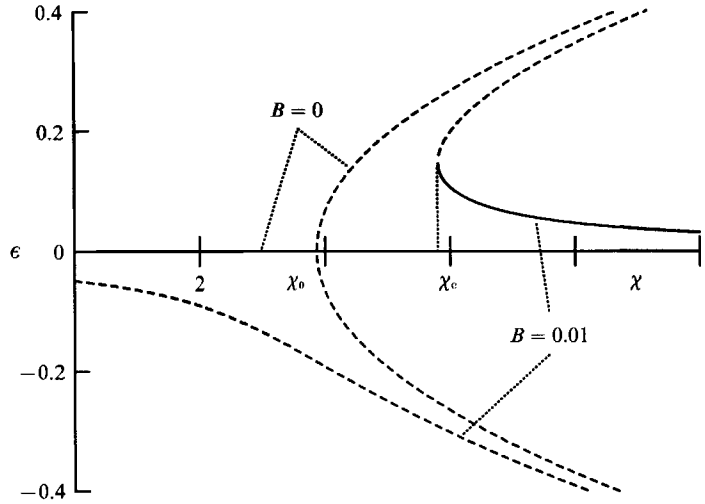

FIGURE 4. Bifurcation diagram in the (ε, χ)-plane for $\beta = 0.55$ and $\Lambda = 4$, showing a pitchfork structure for $B = 0$ and its breaking into two isolated branches for $B = 0.01$. ---, unstable branches and ——, stable branches, except the line $\varepsilon = 0$, which is unstable for $\chi < \chi_0$.

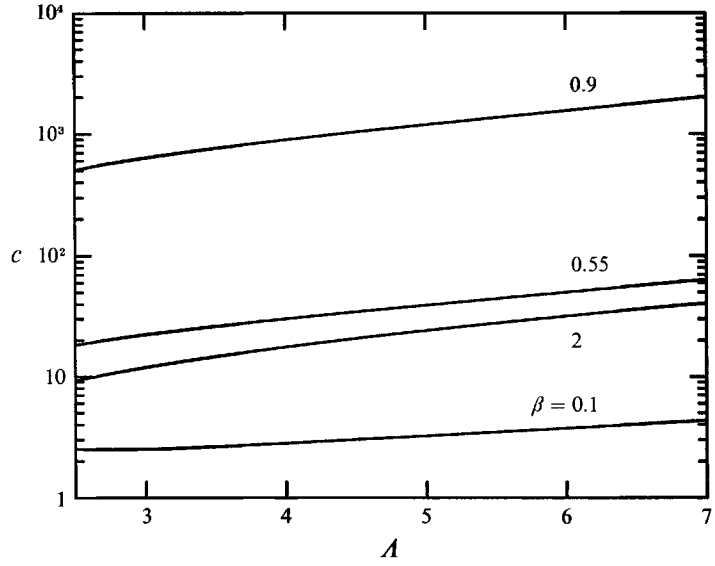

FIGURE 5. Curvature of the parabolic branch versus the slenderness in the bifurcation diagram for $B = 0$ and different β. Parameter $c(\beta, \Lambda)$ is a measure of the sensitivity of the bridge to finite-amplitude perturbations.

The computation of the coefficients ψ_{030} and ψ_{110} indicates that the curvature of the parabolic branch is considerable, as shown in figure 5, where we represent $c \equiv -2\psi_{030}/\psi_{110}$ as a function of Λ for different β. The curvature of the parabola is related to the sensitivity of the liquid bridge to perturbations of finite amplitude. It increases monotonically with Λ and depends strongly on the relative permittivities: it increases as this parameter deviates from unity. Thus, for polarizable configurations not only the electric field necessary for stabilization is smaller but the bridge is less sensitive to finite-amplitude perturbations.

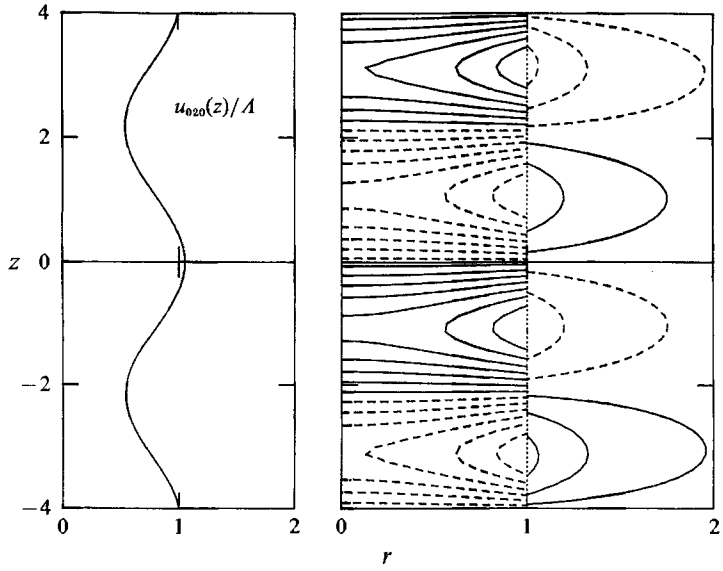

FIGURE 6. Shape and equipotentials given by the functions $u_{020}(z)$ and $\varphi_{020}(r,z)$, the corrections of order ε^2 in the expansion of $f(z)$ and $\phi(r,z)$, respectively.

The computation also gives information about the function $u_{020}(z)$ that appears multiplied by ε^2 in the expansion of $u(z)$ in the parameters ε, $\bar{\chi}$ and B. This term is the lower-order correction to the shape of the interface given by the linear analysis. In figure 6 we plot $u_{020}(z)$ and an equipotential map of the function $\varphi_{020}(r,z)$ for $\beta = 0.55$ and $\Lambda = 4$. The symmetry correlation is apparent.

6.2. *The influence of gravity*

For $B \neq 0$, figure 4 shows the breaking of the pitchfork bifurcation diagram into two isolated branches. The cylindrical bridge is no longer a solution to the full equations. The factorization theorem is still applicable to this latter situation: a change in the stability behaviour at, and only at, the existing turning point is produced. The position of this turning point gives the new minimum electric Bond number for which there exists a solution close to the cylinder. In terms of the coefficients ψ_{030}, ψ_{110} and ψ_{001} the stability criterion is now

$$\chi_c = \chi_0 + \alpha(\Lambda,\beta)B^{\frac{2}{3}}, \quad \alpha(\Lambda,\beta) = -\frac{3}{2^{\frac{2}{3}}}\frac{(\psi_{030}\psi_{001}^2)^{\frac{1}{3}}}{\psi_{110}}. \tag{81}$$

The law $B^{\frac{2}{3}}$ implies that the effect of residual gravity upon the stability of the liquid bridge is not negligible. Moreover, the order of magnitude of the coefficient α is much greater than unity, as shown in figure 7 as a function of Λ for several β. Thus the correction due to gravity, even for low levels, is important. From the figure we observe an increase in the effect of gravity upon the stability of bridges with greater slenderness and fixed B. As a conclusion, longer bridges feel strongly the destabilizing effect of residual axial gravity. The amplitudes of deformation at criticality are defined by

$$\varepsilon_r = \gamma(\Lambda,\beta)B^{\frac{1}{3}}, \quad \gamma(\Lambda,\beta) = \left(\frac{\psi_{001}}{2\psi_{030}}\right)^{\frac{1}{3}}. \tag{82}$$

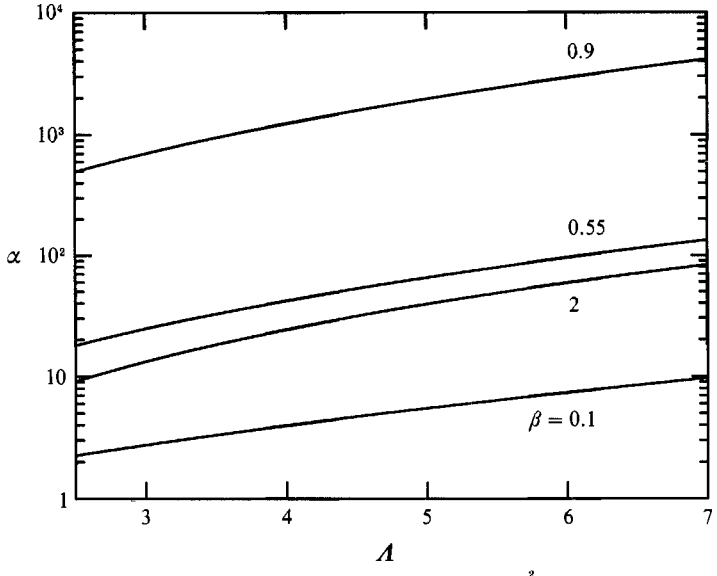

FIGURE 7. Coefficient α in the law $\chi_c = \chi_0 + \alpha B^{\frac{2}{3}}$ *vs.* Λ for different β.

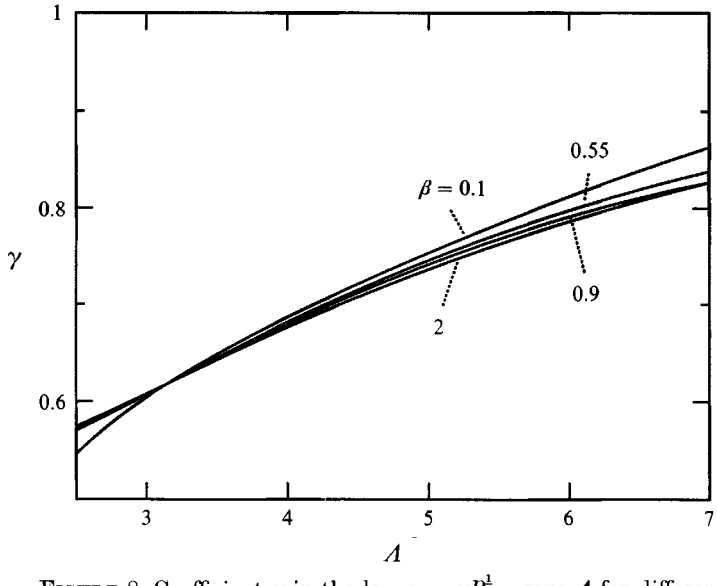

FIGURE 8. Coefficient γ in the law $\varepsilon_c = \gamma B^{\frac{1}{3}}$ versus Λ for different β.

In figure 8 we plot the coefficient γ versus Λ. Obviously, the cylinder is more distorted for greater slendernesses. However, a variation in the relative permittivity does not influence appreciably the critical deformation.

In order to construct the new stability curves it is necessary to know the values $\chi_c(\Lambda, \beta, B)$ for $\Lambda < \pi$. This region is not directly available from (81) unless we also consider the extension of the curves $\chi_0(\beta, \Lambda)$ for negative values (the dashed parts in figure 2). The alternative to this purely mathematical construction is to find the bifurcation equation for fixed χ giving the relationship between the amplitude ε and $\lambda \equiv \Lambda_0(\beta, \chi) - \Lambda$, the deviation of the slenderness with respect to the double point

bifurcation value ($\Lambda_0(\beta,\chi)$ is the inverse function of $\chi_0(\beta,\Lambda)$). We can deduce the bifurcation diagram in the (ε,Λ)-plane from that of the (ε,χ)-plane. It is found that the bifurcation equation for fixed χ has the expansion

$$\varepsilon\left(\frac{\partial\chi}{\partial\Lambda}\psi_{110}\lambda+\psi_{030}\varepsilon^2\right)+\psi_{001}B+\ldots=0, \tag{83}$$

where the functions $\psi_{ijk}(\chi,\Lambda,\beta)$ and $\partial\chi/\partial\Lambda$ are evaluated at $\Lambda_0(\beta,\chi)$.

Both possibilities of construction of the new stability curves in the (χ,Λ)-plane are not equivalent because they represent two ways of truncation of the exact bifurcation equation. The first one leads to a vertical translation of the curve $\chi_0(\beta,\Lambda)$ to give $\chi_c(\beta,\Lambda,B)$. The second one performs a horizontal translation to the left. The decision about which method is better comes from comparison between them for the case $\chi=0$ available in the literature (Coriell, Hardy & Cordes 1977). From (83) we obtain an analytical expression for the stability curve in the following way: the coefficients ψ_{110}, ψ_{001} and ψ_{030} are evaluated using (65) with the functions $h^{(3)}_{110}$, $h^{(3)}_{001}$ and $h^{(3)}_{030}$, respectively (the only necessity for zero applied electric field), which are given in the Appendix A. These functions must be evaluated for $\chi_0=0$. In particular, for $f_0(z)$ and $u_{020}(z)$ we obtain the functions given by Vega & Perales:

$$f_0(z)=c\sin z,\quad u_{020}(z)=-\tfrac{1}{4}c^2\left(1-\cos\frac{2\pi z}{\Lambda}\right), \tag{84}$$

c being some known constant arising from a different normalization. Introducing these functions in (65) we obtain

$$\psi_{001}=2\pi c,\quad \psi_{030}=-\tfrac{3}{2}\pi c^4. \tag{85}$$

On the other hand we have

$$\psi_{110}=2\Lambda\Delta\epsilon\int_{-\Lambda}^{\Lambda}\mathrm{d}z f_0(z)\,\phi_{0,z}(1,z)=-(\Delta\epsilon)^2\Lambda\sum_{\substack{n=1\\ \text{odd}}}^{\infty}\frac{x_n}{H_0(\beta,x_n)\,q_n^2}, \tag{86}$$

where use of (25) and (26) has been made. The factor $\mathrm{d}\chi_0/\mathrm{d}\Lambda$ is given by

$$\frac{\mathrm{d}\chi_0}{\mathrm{d}\Lambda}=-\left.\frac{\partial S_-/\partial\Lambda}{\partial S_-/\partial\chi}\right|_{\chi=\chi_0(\beta,\Lambda)}, \tag{87}$$

with $S_-(\beta,\Lambda,\chi)$ defined in (21). These derivatives are evaluated at $\Lambda=\pi$, $\chi=\chi_0(\beta,\pi)=0$,

$$\frac{\partial S_-}{\partial\chi}=-(\Delta\epsilon)^2\sum_{\substack{n=1\\ \text{odd}}}^{\infty}\frac{x_n}{H_0(\beta,x_n)\,q_n^2}=\frac{\psi_{110}}{\pi}, \tag{88}$$

$$\frac{\partial S_-}{\partial\Lambda}=-\frac{2}{\pi}\sum_{\substack{n=1\\ \text{odd}}}^{\infty}\frac{x_n^2}{q_n^2}=-\frac{2}{\pi^2}\int_{-\pi}^{\pi}\mathrm{d}z f_{0,z}^2=-\frac{2c^2}{\pi}. \tag{89}$$

The resulting bifurcation equation truncated in ε and $\lambda=\pi-\Lambda$ gives the stability criterion

$$\Lambda_c=\pi[1-(\tfrac{3}{2})^{\frac{4}{3}}B^{\frac{2}{3}}], \tag{90}$$

which is in accordance with Vega & Perales' work. This gives confidence about the derivation of (83). However, from the first method of construction of the stability curves we can obtain Λ_c as that value for which $\chi_c=0$ (see figure 9). In table 1 we

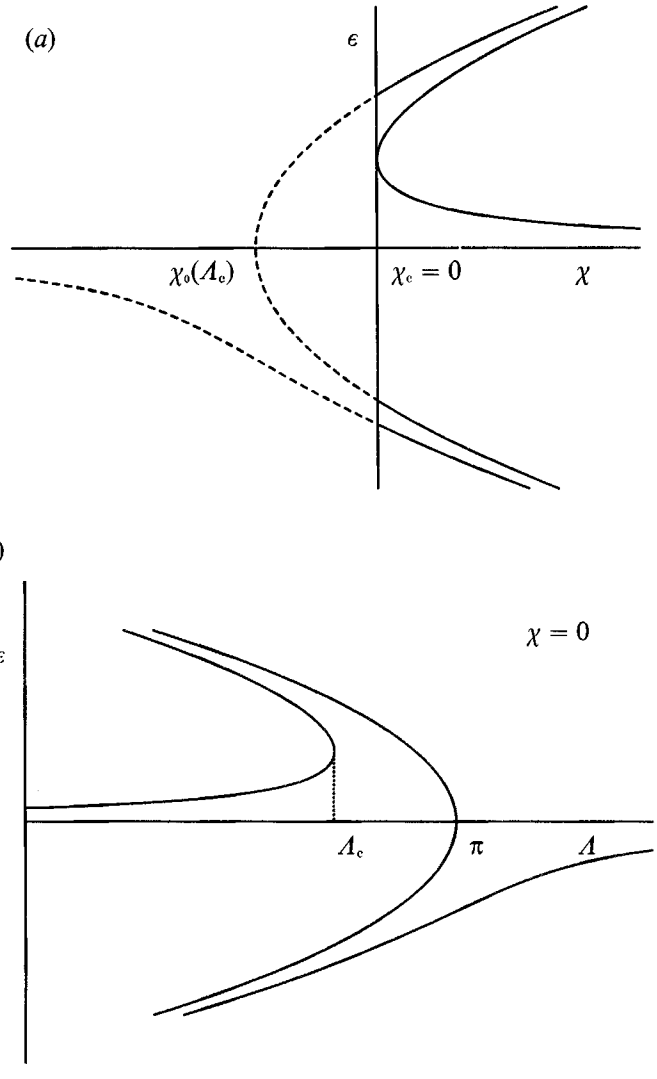

FIGURE 9. Two possible ways to build the stability curves $\chi_c(\beta, \Lambda, B)$ from $\chi_0(\beta, \Lambda)$, particularized for the point $\chi_c = 0$: (*a*) Given $B \neq 0$ there exist some $\Lambda_c < \pi$ such that, in spite of the negative value of $\chi_0(\Lambda_c)$, the isolated branch having the turning point at $\chi_c = 0$ has physical meaning. The solid lines in the bifurcation diagram give true information about admissible stable or unstable equilibrium solutions with and without residual gravity. (*b*) Fixed χ leads to a bifurcation diagram in the (ϵ, Λ)-plane having a turning point whose location determines Λ_c. Both ways are not equivalent (see text).

compare the values given by both methods with numerical data (Coriell *et al.* 1977). The bridge stability in the absence of an electric field is found more accurately with the help of the electrical parameter χ.

In figure 10 we present the stability criteria using vertical translation for different levels of gravity, namely $B = 10^{-3}$, 10^{-2} and 10^{-1}, compared with the curve for $B = 0$ and some available experimental data (González *et al.* 1989). These curves have also been obtained by finite-element techniques valid for arbitrary gravitational Bond number, presented in a companion paper (Ramos & Castellanos 1993). Comparison

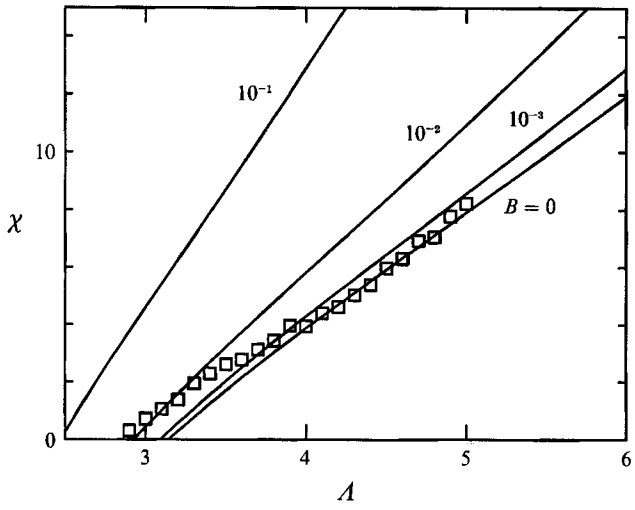

FIGURE 10. Stability curves for different gravitational Bond numbers (including $B = 0$), compared with experimental available data (González *et al.* 1989).

B	Λ_c	Coriell *et al.*	Vega & Perales
0.000258	3.120	3.12	3.119
0.000702	3.100	3.10	3.099
0.00239	3.051	3.05	3.045
0.00722	2.965	2.96	2.940
0.0100	2.928	2.92	2.891
0.0162	2.862	2.85	2.796
0.0200	2.829	2.815	2.744
0.0518	2.639	2.60	2.392
0.100	2.473	2.405	1.979

TABLE 1. Comparison between the critical slenderness for $\chi = 0$ obtained by different methods. The first column shows the gravitational Bond numbers; the other columns gives the corresponding values of Λ_c obtained with the help of an $\varepsilon - \chi$ diagram, by Coriell *et al.* 1977 and by Vega & Perales 1983 (based in an $\varepsilon - \Lambda$ diagram)

between both independent approaches to the problem gives a full agreement up to Bond numbers of the order of 10^{-2} and deviation beyond this order. This determines the range of validity of our perturbative theory.

In the previous work it was suggested that the poor agreement between the curve $B = 0$ and experiments for small slendernesses was due to residual gravity effects. This assertion seems to be correct, but, conversely, the new stability criterion diverges for greater Λ from the experimental data. A possible explanation for this discrepancy may lie in the effect of the metallic rings used to anchor the liquid bridge. The inclusion of this feature in the theoretical model or the use of another anchoring method to avoid electric field singularities may improve the agreement between theory and experiment. On the other hand, as the gravitational Bond number associated to each experimental point was not carefully controlled, we need further experiments to confirm our results quantitatively.

7. Conclusions

It was stated in a previous work that an axial electric field had a stabilizing effect on a cylindrical dielectric liquid bridge. Through the construction of a theoretical model to take into account the effect of residual axial gravity we incidentally found a pitchfork subcritical bifurcation diagram for this configuration, which gives information about its sensitivity to small but finite deformations. The electric field intensity needed to hold stable slightly deformed bridges increases considerably with respect to the linear stability criterion, specially for long liquid bridges.

Axial residual gravity acts as a permanent deforming agent, so that its destabilizing effect is very important. The new stability criterion diverges from that with $B = 0$ as Λ increases, a fact which is in accordance with the above-mentioned sensitivity to small disturbances. This behaviour can be used to measure low acceleration levels with the help of long liquid bridges.

This work has been supported by the Spanish Dirección General Interministerial de Ciencia y Tecnología (DGICYT) under contract PB87-0943.

We wish to thank Dr F. Medina for his help in summation techniques applied in this work.

Appendix A

Functions of z, defined at the linearized interface ($r = 1$), necessary to evaluate the coefficients ψ_{ijk}.

$$h^{(1)}_{020} = -f_0 \Delta\phi_{0,r}, \tag{A 1}$$

$$h^{(2)}_{020} = -f_0 \Delta(\epsilon\phi_{0,rr}) + f_{0,z} \Delta(\epsilon\phi_{0,z}), \tag{A 2}$$

$$\begin{aligned} h^{(3)}_{020} = {} & f_0^2 - (\tfrac{1}{2} + \chi_0 \Delta\epsilon) f_{0,z}^2 + 2\Lambda^2 \chi_0 \Delta(\epsilon\phi_{0,z}^2) \\ & - 2\Lambda^2 \chi_0 \Delta(\epsilon\phi_{0,r}^2) + 2\Lambda\chi_0 f_0 \Delta(\epsilon\phi_{0,zr}) + 4\Lambda\chi_0 \phi_{0,\zeta} \Delta(\epsilon\phi_{0,r}), \end{aligned} \tag{A 3}$$

$$h^{(4)}_{020} = -\tfrac{1}{2} f_0^2, \tag{A 4}$$

$$h^{(1)}_{030} = -u_{020} \Delta\phi_{0,r} - \tfrac{1}{2} f_0^2 \Delta\phi_{0,rr} - f_0 \Delta\varphi_{020,r}, \tag{A 5}$$

$$\begin{aligned} h^{(2)}_{030} = {} & -u_{020} \Delta(\epsilon\phi_{0,rr}) - \tfrac{1}{2} f_0^2 \Delta(\epsilon\phi_{0,rrr}) - f_0 \Delta(\epsilon\varphi_{020,rr}) \\ & + f_{0,z} f_0 \Delta(\epsilon\phi_{0,zr}) + f_{0z} \Delta(\epsilon\varphi_{020,z}) + u_{020,z} \Delta(\epsilon\phi_{0,z}), \end{aligned} \tag{A 6}$$

$$\begin{aligned} h^{(3)}_{030} = {} & -f_0^3 + 2 f_0 u_{020} - (1 + 2\chi_0 \Delta\epsilon) f_{0,z} u_{020,z} \\ & + \tfrac{3}{2} f_{0,zz} f_{0,z}^2 + \tfrac{1}{2} f_0 f_{0,z}^2 - 4\Lambda^2 \chi_0 f_0 \Delta(\epsilon\phi_{0,r} \phi_{0,rr}) \\ & - 4\Lambda^2 \chi_0 \Delta(\epsilon\phi_{0,r} \varphi_{020,r}) + 4\Lambda\chi_0 u_{020,z} \Delta(\epsilon\phi_{0,r}) \\ & + 8\Lambda^2 \chi_0 f_{0,z} \Delta(\epsilon\phi_{0,r} \phi_{0,z}) + 4\Lambda\chi_0 f_0 f_{0,z} \Delta(\epsilon\phi_{0,rr}) \\ & + 4\Lambda\chi_0 f_{0,z} \Delta(\epsilon\varphi_{020,r}) + 4\Lambda^2 \chi_0 f_0 \Delta(\epsilon\phi_{0,z} \phi_{0,zr}) \\ & + 2\Lambda\chi_0 u_{020} \Delta(\epsilon\phi_{0,zr}) + \Lambda\chi_0 f_0^2 \Delta(\epsilon\phi_{0,zrr}) \\ & + 2\Lambda\chi_0 f_0 \Delta(\epsilon\varphi_{020,zr}) + 4\Lambda^2 \chi_0 \Delta(\epsilon\phi_{0,z} \varphi_{020,z}) \\ & - 4\Lambda\chi_0 f_{0,z}^2 \Delta(\epsilon\phi_{0,z}), \end{aligned} \tag{A 7}$$

$$h^{(4)}_{030} = -f_0^2 u_{020}, \tag{A 8}$$

$$h^{(1)}_{110} = h^{(2)}_{110} = h^{(4)}_{110} = 0, \quad h^{(3)}_{110} = \frac{\Delta\epsilon}{2\Lambda} \phi_{0,z}, \tag{A 9}$$

$$h^{(1)}_{001} = h^{(2)}_{001} = h^{(4)}_{001} = 0, \quad h^{(3)}_{001} = z. \tag{A 10}$$

Appendix B

$$12h\boldsymbol{D}^{1u} = \begin{array}{c} \\ 1 \\ 2 \\ \vdots \\ n-1 \\ n \end{array} \begin{array}{c} \begin{array}{ccccccccccc} 0 & 1 & 2 & 3 & 4 & \dots & n-4 & n-3 & n-2 & n-1 & n \end{array} \\ \begin{pmatrix} -8 & 1 & 8 & -1 & & & & & & & \\ 1 & -8 & 0 & 8 & -1 & & & & & & \\ & & & & & \ddots & & & & & \\ & & & & & & 1 & -8 & 0 & 8 & -1 \\ & & & & & & & -1 & 6 & -18 & 10 \end{pmatrix} \end{array} \tag{B 1}$$

$$12h\boldsymbol{D}^{1\varphi} = \begin{array}{c} \\ 0 \\ 1 \\ 2 \\ 3 \\ \vdots \\ n-1 \\ n \end{array} \begin{array}{c} \begin{array}{ccccccccccc} 1 & 2 & 3 & 4 & 5 & \dots & n-4 & n-3 & n-2 & n-1 & n \end{array} \\ \begin{pmatrix} 16 & -2 & & & & & & & & & \\ -1 & 8 & -1 & & & & & & & & \\ -8 & 0 & 8 & -1 & & & & & & & \\ 1 & -8 & 0 & 8 & -1 & & & & & & \\ & & & & & \ddots & & & & & \\ & & & & & & 1 & -8 & 0 & 8 & -1 \\ & & & & & & & -1 & 6 & -18 & 10 \end{pmatrix} \end{array} \tag{B 2}$$

$$12h^2\boldsymbol{D}^{2u} = \begin{array}{c} \\ 0 \\ 1 \\ 2 \\ \vdots \\ n-2 \\ n-1 \\ n \end{array} \begin{array}{c} \begin{array}{ccccccccccc} 0 & 1 & 2 & 3 & 4 & \dots & n-4 & n-3 & n-2 & n-1 & n \end{array} \\ \begin{pmatrix} -30 & 32 & -2 & & & & & & & & \\ 16 & -31 & 16 & -1 & & & & & & & \\ -1 & 16 & -30 & 16 & -1 & & & & & & \\ & & & & & \ddots & & & & & \\ & & & & & & -1 & 16 & -30 & 16 & -1 \\ & & & & & & & -1 & 16 & -30 & 16 \\ & & & & & & & -1 & 4 & 6 & -20 \end{pmatrix} \end{array} \tag{B 3}$$

$$12h^2\boldsymbol{D}^{2\varphi} = \begin{array}{c} \\ 1 \\ 2 \\ 3 \\ \vdots \\ n-2 \\ n-1 \\ n \end{array} \begin{array}{c} \begin{array}{ccccccccccc} 1 & 2 & 3 & 4 & 5 & \dots & n-4 & n-3 & n-2 & n-1 & n \end{array} \\ \begin{pmatrix} -1 & 16 & -1 & & & & & & & & \\ -29 & -30 & 16 & -1 & & & & & & & \\ 16 & 16 & -30 & 16 & -1 & & & & & & \\ & & & & & \ddots & & & & & \\ & & & & & & -1 & 16 & -30 & 16 & -1 \\ & & & & & & & -1 & 16 & -30 & 16 \\ & & & & & & & -1 & 4 & 6 & -20 \end{pmatrix} \end{array} \tag{B 4}$$

REFERENCES

COLLIN, R. E. 1991 *Field Theory of Guided Waves*. New York: IEEE Press.

CORIELL, S. R. & CORDES, M. R. 1977 Theory of molten zone shape and stability. *J. Cryst. Growth* **42**, 466–472.

CORIELL, S. R., HARDY, S. C. & CORDES, M. R. 1977 Stability of liquid zones. *J. Colloid Interface Sci.* **60**, 126–136.

GONZÁLEZ, H. & CASTELLANOS, A. 1990 The effect of an axial electric field on the stability of a rotating dielectric cylindrical liquid bridge. *Phys. Fluids* A **2**(11), 2069–2071.

GONZÁLEZ, H., MCCLUSKEY, F. M. J., CASTELLANOS, A. & BARRERO, A. 1989 Stabilization of dielectric liquid bridges by electric fields in the absence of gravity. *J. Fluid Mech.* **206**, 545–561.

GRANEY, L. & RICHARDSON, A. A. 1981 The numerical solution of non-linear partial differential equations by the method of lines. *J. Comput. Appl. Maths* **7**(4), 229–235.

IOOSS, G. & JOSEPH, D. D. 1980 *Elementary Stability and Bifurcation Theory*. Springer.

MARTÍNEZ, I. 1983 Stability of axisymmetric liquid bridges. In *Material Sciences under Microgravity*, ESA SP-191, pp. 267–273.

MIKHAIL, N. M. 1987 On the validity and stability of the method of lines for the solution of partial differential equations. *Appl. Maths Comput.* **22**, 89–98.

MYSHKIS, A. D., BABSKII, V. G., KOPACHEVSKII, N. D., SLOBOZHANIN, L. A. & TYUPSOV, A. D. 1987 *Low-gravity Fluid Mechanics*. Springer.

PERALES, J. M. 1987 Non-axisymmetric effects on long liquid bridges. *Acta Astronautica* **15**(8), 561–565.

PERALES, J. M., SANZ, A. & RIVAS, D. 1990 Eccentric rotation of a liquid bridge. *Appl. Microgravity Tech.* **2**(4), 193–197.

RAMOS, A. & CASTELLANOS, A. 1993 Bifurcation diagrams of axisymmetric liquid bridges of arbitrary volume in electric and gravitational axial fields. *J. Fluid Mech.* **249**, 207–225.

VEGA, J. M. & PERALES, J. M. 1983 Almost cylindrical isorotating liquid bridges for small Bond numbers. In *Material Sciences under Microgravity*, ESA SP-191, pp. 247–252.